ACS APPLIED POLYMER MATERIALS

pubs.acs.org/acsapm

Letter

Remote Loading of Gas Bubbles into Polylactic Acid Microcapsules Creates Acoustically Active Janus Particles

Arvin Honari, Pallavi S. Kapilavaih, Nasrin Akter, and Shashank R. Sirsi*

Cite This: *ACS Appl. Polym. Mater.* 2022, 4, 773−780

Read Online

ACCESS | Metrics & More | Article Recommendations | Supporting Information

ABSTRACT: Polymeric microcapsules (MCs) are biocompatible agents used in biomedical applications such as drug delivery and in vivo imaging. We have discovered a method of remotely loading air into polylactic acid (PLA)-based MCs with an aqueous core. When the microcapsules are suspended in high content glycerol and propylene glycol solutions, changes in gas solubility cause bubbles to nucleate within the core through an "Ouzo-like" effect. The resulting bubble displaces the internal fluid of the MCs, but small molecules are retained in their interior. The residual content does not homogeneously distribute; rather, it localizes to one specific location, creating gas-filled Janus particles.

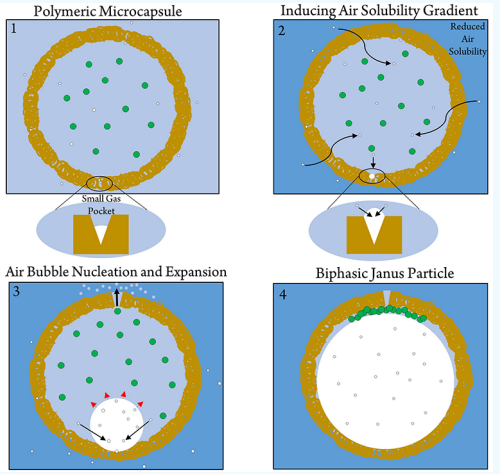

KEYWORDS: *polymeric microcapsules, microbubbles, Janus particles, ultrasound, bubble nucleation*

Polymeric microcapsules (MCs) are aqueous reservoirs protected by soft or rigid polymeric shells. MCs are particularly well-suited for encapsulating both hydrophobic and hydrophilic molecules. Their ease of manufacturing, high loading capacity, and effective protection against enzymatic degradation and leakage of the encapsulated material make them highly attractive for in vivo biomedical applications.[1,2]

Polymeric MCs can be made acoustically active by the introduction of gas bubbles into their core, thus enabling the development of multimodal and theranostic ultrasound contrast agents (UCAs). Gas bubbles are well-known UCAs that respond to ultrasound by volumetrically oscillating.[3] This phenomenon occurs due to the compressibility of gas, compared to that of a liquid medium.[4] This unique behavior of bubbles has been used for a variety of applications, especially in biomedical engineering.[5]

A few groups have successfully made polymer MCs acoustically active for imaging or delivery applications. The Wheatley group developed a method of formulating polymer-shelled microbubbles from MCs for imaging and therapy.[6,7] They used a double emulsion approach to generate PLA and PLGA-based MCs, followed by a freeze-drying process to sublime water and poragens that generate a gas bubble. The sublimation process can take up to 72 h and requires high amounts of energy. Later research from this group used the same ultrasound contrast agents for drug delivery by incorporating doxorubicin on, within, or inside the polymeric shell.[8] Wrenn *et al.* demonstrated an alternative approach for making MCs acoustically active by encapsulating lipid-coated microbubbles in calcein-loaded polymeric MCs.[9,10] However, the ultrasound response of the lipid bubbles is significantly diminished due to their confinement within a polymeric shell as well as the lipid coating. More recently, Peng et al. formulated caged microbubbles using a nanoprecipitation method to trap bubbles in a porous polymeric shell.[11,12]

In the present study, we developed a method of nucleating bubbles in MCs by remote loading of gas using a simple one-step procedure. Remote, or active loading, is a technique widely used for loading drugs into a carrier, typically by creating a transmembrane gradient that drives small molecules through the carrier shell.[13] This study was in part motivated by recent research in the ultrasound contrast agent field using the "Ouzo" effect to nucleate perfluorocarbon droplets in the core of liposomes.[14] The classic Ouzo effect is seen in ternary mixtures of water, a type of oil, and a type of alcohol. When

Received: November 8, 2021
Accepted: December 22, 2021
Published: January 19, 2022

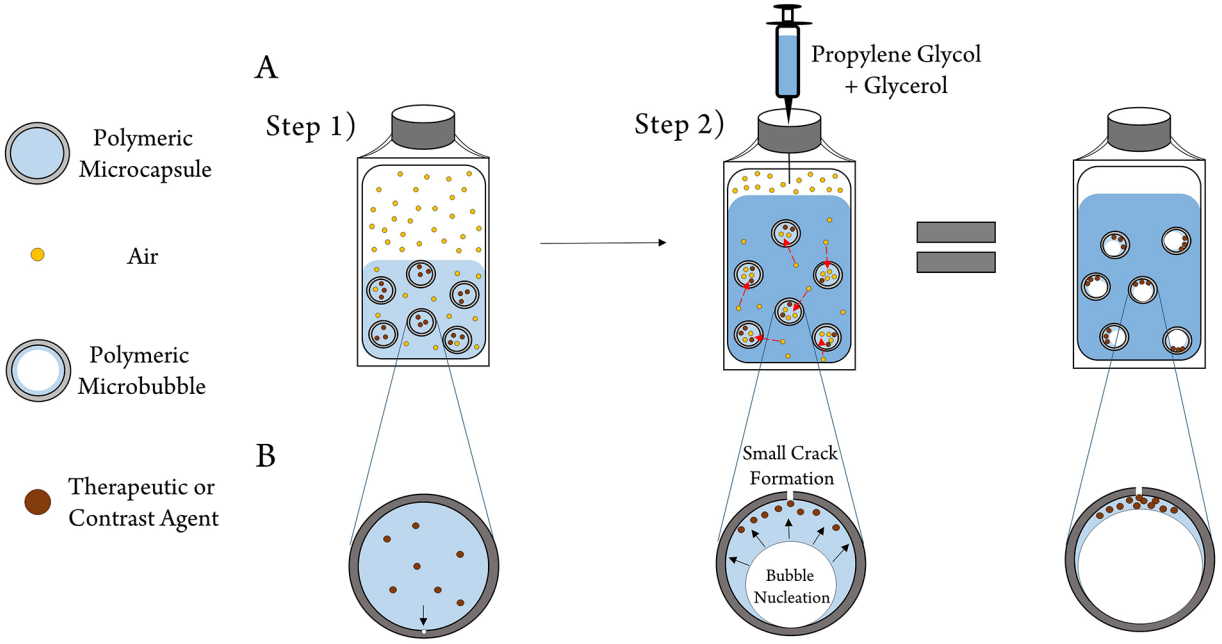

Figure 1. Experimental procedure for generating acoustic vesicles. (A) Schematic for producing acoustic vesicles by altering the solubility gradient across the shell. By adding propylene glycol and glycerol, the solubility of air will be reduced, driving air into the core of the microcapsule. In step 1, microcapsules are suspended in water, and in step 2, propylene glycol and glycerol are introduced, creating a transmembrane solubility gradient. Gas bubbles will nucleate within the capsule core, creating acoustic vesicles. (B) Proposed mechanism of Janus particle formation. We speculate that the nucleation starts from small gas pockets within the polymeric shell (shown with a small arrow in step 1). In step 2, propylene glycol and glycerol are introduced to induce the transmembrane solubility gradient across the PLA shell, which eventually causes air to diffuse into the core. Bubble nucleation forces water out through small cracks or pores caused by pre-existing shell defects or increasing internal pressure; however, larger and less permeable molecules cannot physically diffuse and will accumulate at the exit point. The final product is a gas-filled PLA microbubble with residual internal content accumulated at a single point, creating Janus-like particles.

water is added to a mixture of oil and alcohol, the oil solubility in the mixture decreases, driving nucleation of small stable droplets that form a stable emulsion. The "Ouzo" method is an easy approach to make emulsions for drug carrier synthesis without the need for surfactants or vigorous mixing.[15]

Here, we proposed a similar method of altering the solubility gradient between the external and internal environment of MCs. Our rationale was that suspending PLA MCs in an aqueous solution with low air solubility would drive gas into the vesicles' water core. We selected propylene glycol (PPG) and glycerol as excipients to lower air solubility as nitrogen and oxygen solubilities are considerably less in glycerol and PPG solutions compared to pure water (nitrogen is ∼2.5 times less soluble in 30% glycerol and ∼1.5 times less soluble in 30% PPG).[16−18] Furthermore, both nitrogen and oxygen are small molecules that are known to be permeable to thin PLA films.[19] According to our hypothesis, reduction of air solubility in the surrounding solution drives air into the aqueous core of MCs and initiates the nucleation of gas bubbles. The final product is a gas-loaded PLA MC that we call an acoustic vesicle (Figure 1).

As confirmed by microscopy, we were able to generate gas-loaded MCs by simply suspending MCs in 30% PPG and 30% glycerol concentrations. Furthermore, MCs with larger gas bubbles are buoyant and rise to the coverslip. However, MCs with smaller bubbles, thicker PLA shells, or no bubbles are not buoyant enough to overcome the weight of the PLA shell (Figure 2A).

We reasoned that increasing the concentration of PPG and glycerol would increase the degree of nucleation proportionally by lowering gas solubility. To test this hypothesis, we resuspended the MCs at varying concentrations of PPG and glycerol. The results shown in panels B and C in Figure 2 confirmed our hypothesis: by increasing the concentration of PPG and glycerol, we saw an increased number of bubble-loaded MCs. Although it seems that increasing PPG and glycerol content above 30% decreases the number of bubbles beneath the coverslip, this discrepancy is due to the high viscosity of the solution and the inability of the bubbles to rise to the top. A significant number of neutrally buoyant bubbles can be seen throughout the sample. Thus, the number of bubbles counted on top of the sample reported in Figure 2B is not representative of the total number of bubbles. We chose 30% PPG and 30% glycerol solution for the following experiments because of the ease of handling in the less viscous medium.

To further confirm the nucleation hypothesis, we also produced acoustic vesicles using deionized water and ethanol because nitrogen solubility in water is almost 18 times less compared to ethanol.[16] MCs were resuspended in ethanol and then water was added to the system to drive nucleation. We saw an increase in the number of nucleation events in the MCs, as ethanol concentration increased. However, because ethanol is a poor solvent for PLA, we observed high levels of MC aggregation after a few hours (Figure S1).

To show that the nucleation events are primarily due to a transmembrane solubility gradient rather than pressure or mixing, we embedded PLA MCs in 1% agarose hydrogel. The gel was placed in a perfusion chamber containing only air and water. Water was exchanged with a 30% PPG, 30% glycerol 1×

https://doi.org/10.1021/acsapm.1c01562
ACS Appl. Polym. Mater. 2022, 4, 773−780

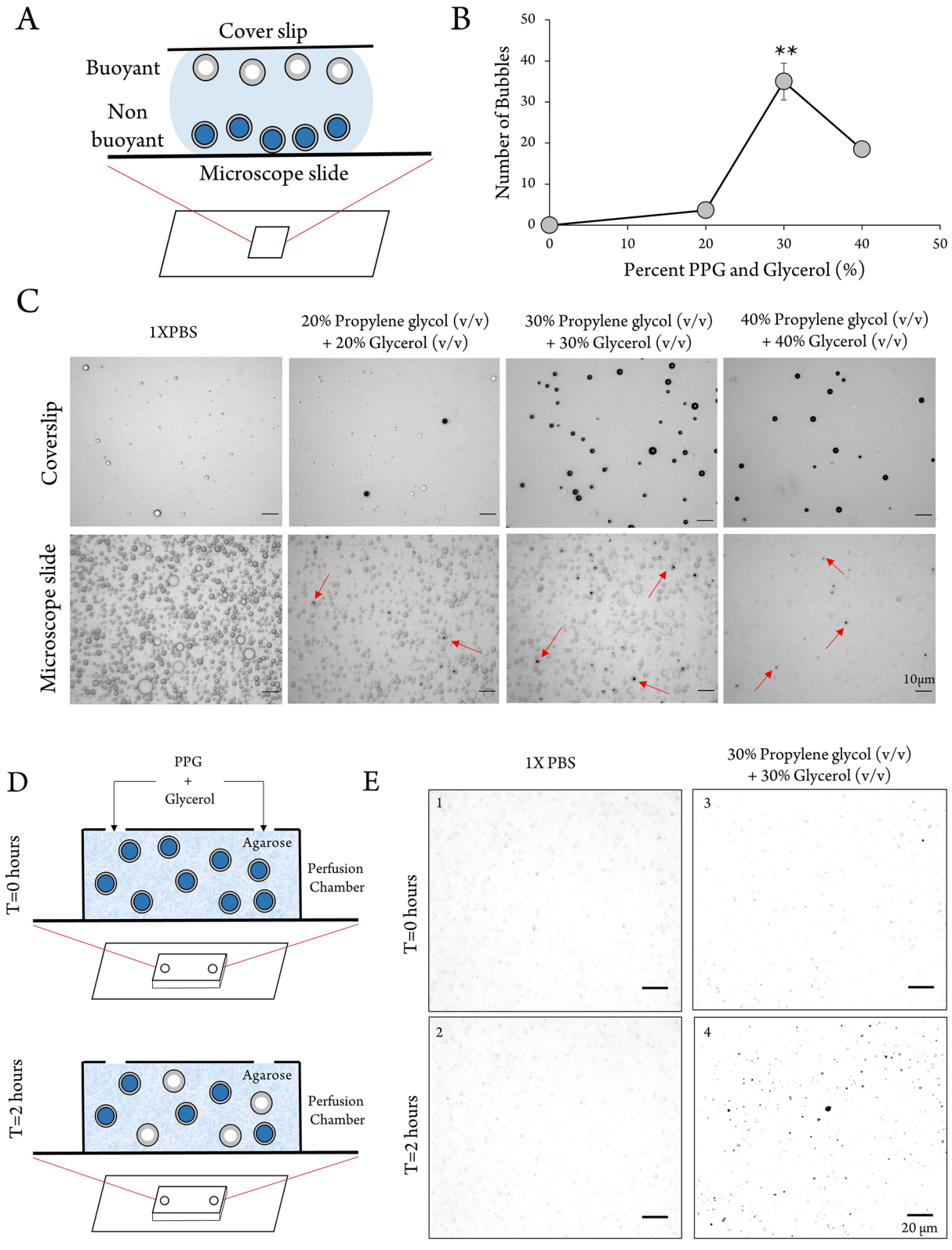

Figure 2. Bubble nucleation using PPG and glycerol. (A) Schematic of a bubble-loaded microcapsule sample on a microscope slide. Bubble-loaded acoustic vesicles are buoyant and will float to the top, beneath the coverslip. However, polylactic acid (PLA) capsules are heavier and will sink to the microscope slide. (B) Average number of bubbles counted beneath the coverslip ($N = 3$). The number of bubbles using 30% PPG and glycerol is significantly higher than 0%, 20%, and 40% ($p < 0.001$ for each group). (C) Example microscopy images show that increasing the PPG and glycerol concentrations increases the number of buoyant particles beneath the coverslip. PLA capsules loaded with smaller bubbles can be seen on the slide, highlighted with red arrows. All scale bars = 10 μm. (D) Schematic of a perfusion chamber with gel-embedded MCs. Microcapsules are embedded in agarose, then PPG and glycerol solutions are perfused in the system. (E) Results from the time-lapse video of bubble nucleation in polylactic acid microcapsules. The images are thresholded to clearly show bubbles as black. The left column shows microcapsules that were

https://doi.org/10.1021/acsapm.1c01562
ACS Appl. Polym. Mater. 2022, 4, 773−780

Figure 2. continued

incubated in 1× PBS (control) with no PPG or glycerol additives. The right column shows microcapsules that were incubated with PPG and glycerol. Bubble nucleation is observed over 2 h. All scale bars = 20 μm.

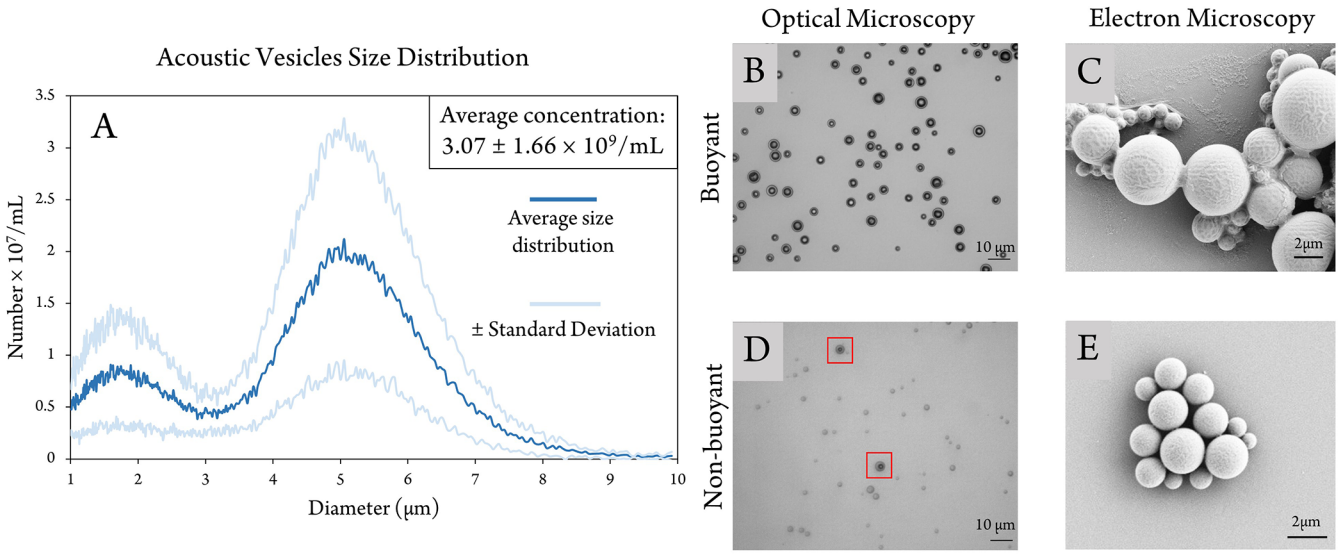

Figure 3. Size and surface characterization of acoustic vesicles. (A) Average size distribution (dark blue) and average concentration of acoustic vesicles after buoyancy separation (N = 3). Light blue lines show a single standard deviation from the mean. (B) Microscopic pictures of separated acoustic vesicles from the coverslip. Acoustic vesicles will float to the top because of their buoyancy and neutrally buoyant or nonbuoyant microcapsules will sink to the microscopic slide. (C) Scanning electron microscopy (SEM) of separated bubbles. (D) Microcapsules that are not loaded with bubbles and microcapsules with smaller gas bubbles can be seen on the microscope slide (shown in red squares). (E) SEM images from non-bubble-loaded microcapsules after washing.

PBS solution, or 1× PBS alone as control (Figure 2D). Live videos were captured to observe the occurrence of nucleation events over time as the glycerol and PPG solution diffused through the gel (Videos S1a and S1b). Figure 2E shows the gas nucleation in MCs over time. This is an indication of the effect of PPG and glycerol on inducing air supersaturation and the onset of nucleation in PLA MCs. It is important to mention that in this particular experiment, the MCs were embedded in a gel, requiring additional time for PPG and glycerol to exchange in the chamber. Therefore, the kinetics of nucleation observed here does not represent the required time to generate bubbles in an aqueous suspension. The nucleation process can be expedited by vortex mixing of the MCs, PPG, and glycerol solution. In all other experiments, we vortex mixed the solution for 5 s and saw comparable degrees of nucleation.

As mentioned earlier, after suspending in PPG and glycerol, the resulting sample consists of both acoustic vesicles and normal non-gas-containing MCs. We separated MCs from acoustic vesicles by differential centrifugation. The resulting size distribution was characterized using a Coulter counter. The size distributions and the concentration of the separated acoustic vesicles are shown in Figure 3A. Acoustic vesicles generated by bubble nucleation are less than 10 μm with a peak at 4.9 μm. The average concentration of the acoustic vesicles sample is 3.07 ± 1.66 × 10^9, which is a comparable yield to conventional methods such as freeze-drying. The concentration of acoustic vesicles can be improved by increasing the PPG and glycerol content or simply using a greater number of MCs when nucleating air bubbles. The shoulder seen in the size distribution graph from 1 to 3 μm is associated with smaller non-gas-loaded MCs. On the basis of microscopy images, acoustic vesicles are bigger compared to MCs. This observation is likely due to the increased buoyancy of larger acoustic vesicles. Small acoustic vesicles may be neutrally buoyant, and thus centrifugation cannot effectively separate them from MCs. It is worth mentioning that centrifugation parameters were not optimized in this study, and this technique leads to some loss of the acoustic vesicles in the process.

Separating acoustic vesicles and MCs allows us to study the gas-loaded particles in more detail. One of our concerns was the fate of small molecules loaded in the core of the MC following a nucleation event, and whether they are retained in the capsule. For this letter, we considered packaging calcein in the MCs as a surrogate drug or imaging agent to demonstrate proof-of-principle of small molecule retention. Calcein is widely used as a surrogate drug because of its fluorescent and auto quenching properties.[20]

Calcein retention in acoustic vesicles was confirmed by confocal microscopy (Figure 4A). It was found that nucleation of air bubbles will expel water but retain calcein solution in the core. Interestingly, the calcein is not equally distributed but accumulates in a single region, or "cap", of the acoustic vesicle. This resulting distribution of calcein creates a Janus particle that is, to the best of our knowledge, unique compared to other acoustic bubbles. Figures 4B,C,D are magnified confocal images to better demonstrate the biphasic Janus particles.

We measured calcein loading in the acoustic vesicles using calcein fluorescence intensity. We extracted calcein using dichloromethane and quantified the amount of calcein before and after extraction.[21] As demonstrated in Figure 4E, the calcein fluorescence intensity increases significantly after the

https://doi.org/10.1021/acsapm.1c01562
ACS Appl. Polym. Mater. 2022, 4, 773−780

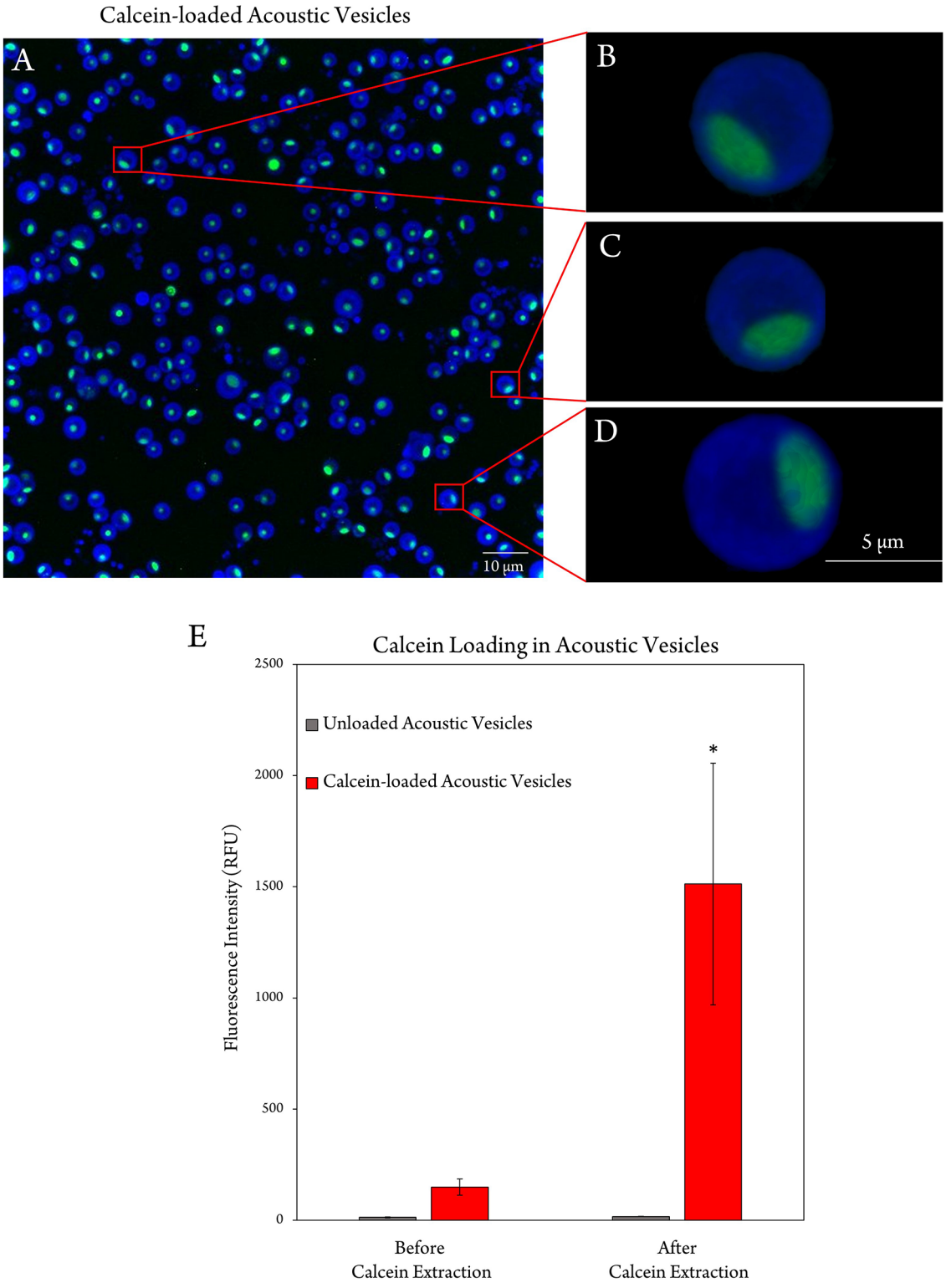

Figure 4. Confocal microscopy of calcein-loaded acoustic vesicles. The accumulation of calcein at one site in the inner polylactic acid capsule shows that small molecules can be retained in the microcapsule after bubble nucleation. (A) Calcein can be seen in all acoustic vesicles, localized in a single region (Z-projections). (B–D) Magnified confocal images of calcein-loaded acoustic vesicles. (E) Calcein loading within the acoustic vesicles was confirmed by calcein fluorescence intensity measurements after dichloromethane extraction. $N = 3$ and $p < 0.01$.

extraction of calcein ($p < 0.01$). This is due to the unloading of encapsulated calcein and subsequent dequenching. The calcein fluorescence intensity before extraction is indicative of quenched calcein entrapped in acoustic vesicles.[20] The concentration of calcein retained in acoustic vesicles was measured at 58.27 μM using a standard linear calcein concentration curve. These results show that calcein is successfully retained within acoustic vesicles. We are extrapolating this finding to suggest that a variety of drugs or contrast agents can be loaded on acoustic vesicles for

https://doi.org/10.1021/acsapm.1c01562
ACS Appl. Polym. Mater. 2022, 4, 773–780

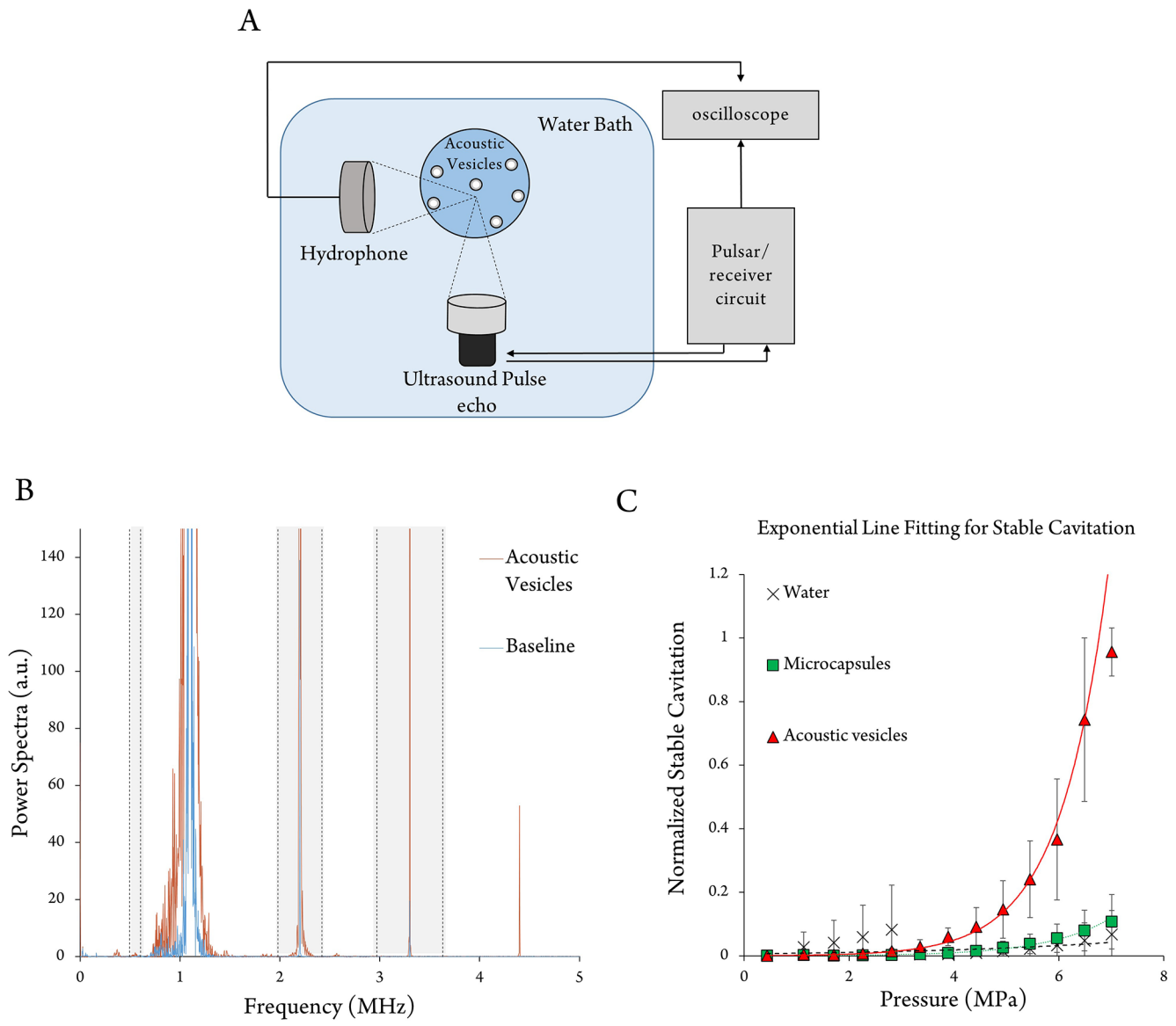

Figure 5. Ultrasound response from acoustic vesicles. (A) Schematic of the setup used for acquiring acoustic data. (B) Example frequency response of acoustic vesicles (orange) compared to baseline (blue) measured using the hydrophone. Shaded light gray areas are where the stable cavitation dosage is calculated using the area under the curve. (C) Summary of normalized stable cavitation doses from acoustic vesicles, MCs, and water at varying pressures (N = 3 per group). Data from each trial is normalized to the stable caviation dosage at the maximum pressure.

therapeutic interventions and/or imaging applications. The distribution of the encapsulated molecules can provide unique applications, especially in drug delivery or imaging. For instance, concentrating particles within the vesicles can potentially induce a chemical reaction, alter the response to energy or excitation wavelength, or even change the release kinetics from acoustic vesicles.

Finally, we demonstrated that gas-loaded MCs were in fact acoustically active. For this purpose, we used a custom chamber, equipped with a focused ultrasound transducer and a hydrophone, to detect the acoustic response from the gas-loaded MCs (Figure 5A). We observed that, unlike MCs and water samples, acoustic vesicles exhibit a harmonic frequency response unique to bubbles when acoustically excited (Figure 5B). As demonstrated in Figure 5C, an increase in acoustic vesicles' stable cavitation dose was observed with increasing ultrasound pressure. The total cavitation for acoustic vesicles, defined by the area under the exponential fit curves in Figure 5B, was significantly higher than that for MCs ($p < 0.005$) and water alone ($p < 0.005$), demonstrating that gas-loaded MCs become acoustically activated. The total cavitation doses for MCs and water were not statistically different ($p = 0.322$). It is worth mentioning that acoustic testing was performed on an unwashed sample with gas-loaded and empty MCs together, and thus only a fraction of the sample would be acoustically active.

The acoustic vesicles developed in the study are not optimized for imaging applications, and hence their acoustic signals are weak compared to freeze-dried hollow MCs (data not shown). One way to improve acoustic vesicles' cavitation is by using poragens in the polymer shell to induce more cracks and defects. This method was used by El-Sherif et al. for optimizing the acoustic response of hollow MCs.[6]

At last, we present a hypothesis for the mechanism by which bubbles nucleate inside polymeric MCs. Nucleation can be defined as the growth of a new phase embryo within another

https://doi.org/10.1021/acsapm.1c01562
ACS Appl. Polym. Mater. 2022, 4, 773−780

phase. According to nucleation theories, bubble nucleation is favored by impurities in the system that drastically lower the energy barrier for nucleation.[22] One of the mentioned impurities is small cavities on the surface of solid boundaries, which can act as gas nucleation sites within a liquid medium[23] and can initiate heterogeneous air nucleation based on mechanisms explained by Jones et al.[24,25]

We hypothesize that a PLA microcapsule wall can act as a solid boundary that provides gas cavities for successful bubble nucleation. After decreasing the solubility of air, local air supersaturation in the periphery of the polymeric shell can initiate heterogeneous nucleation of air bubbles at the cracks on the PLA shell, and eventually, the PLA shell will stabilize the nucleated bubble.

Per our hypothesis, two major considerations need to be addressed to have successful nucleation inside MCs. (1) It is established that supersaturation is necessary for any type of nucleation to occur.[26,27] Classic nucleation theory in supersaturated solutions indicates that if the radius of a gas embryo is beyond the critical embryo radius (R'^*) that embryo can act as a nucleation site and a gas bubble can grow from that small gas pocket.[28,29] R'^* is dependent on the surface tension of the liquid and the degree of supersaturation:

$$R'^* = \frac{2\sigma}{\Delta g v} \tag{1}$$

where σ is the surface tension and $\Delta g v$ is the bulk free energy per unit of liquid volume, associated with transferring molecules to the new phase. $\Delta g v$ is directly dependent on the degree of supersaturation. By adding a solution where air solubility is less than the primary solvent (in our case, propylene glycol and glycerol to water), we will induce supersaturation in the system, increasing the probability of nucleation by reducing the critical embryo radius, R'^*.

(2) The second consideration is the MC shell's gas permeability. Gas permeability is important because the gas molecules can migrate through the polymer shell and find their way to the small pockets of gas on or in between the inner polymeric shell. PLA polymer was chosen for MC production because of its relatively high permeability to gas and vapors as well as biocompatibility.[19]

In conclusion, loading bubbles within MCs and sensitizing them to ultrasound opens up new applications for polymeric MCs such as ultrasound-mediated drug delivery, ultrasound imaging contrast enhancement, or stable poragens for tissue scaffolds. We have developed a method for nucleating gas bubbles into polymeric MCs remotely, generating acoustic vesicles. This method drastically reduces the time and energy required to produce acoustically active polymeric capsules. We plan to investigate the mechanisms of nucleation in more detail by examining the internal surface structure of the MCs. A better understanding of the causes of nucleation can enable more efficient production of acoustic MCs and help generate next-generation MCs for biomedical applications.

■ ASSOCIATED CONTENT

Supporting Information

The Supporting Information is available free of charge at https://pubs.acs.org/doi/10.1021/acsapm.1c01562.

Materials and methods, experimental details, optical microscopy images from nucleation by ethanol and water, and optical microscopy images from nucleation in PLGA microcapsules (PDF)

Video S1a, time-lapse video from bubble nucleation in microcapsules embedded in agarose with 30% PPG and 30% glycerol perfused into the chamber (AVI)

Video S1b, time-lapse video from bubble nucleation in microcapsules embedded in agarose with 1× PBS perfused into the chamber (AVI)

Video S2a, acoustic radiation force on acoustic vesicles in a cellulose capillary tube. The acoustic vesicles at the top of the capillary tube respond to ultrasound (at 1 s) and are pushed to the capillary tube wall through radiation forces (AVI)

Video S2b, acoustic radiation force on non-gas loaded microcapsules in a cellulose capillary tube shows that microcapsules at the bottom of the capillary tube are not responsive to ultrasound (AVI)

■ AUTHOR INFORMATION

Corresponding Author

Shashank R. Sirsi − *Department of Bioengineering, Erik Jonsson School of Engineering, The University of Texas at Dallas, Richardson, Texas 75080, United States;* orcid.org/0000-0002-6390-4379; Email: Shashank.Sirsi@UTDallas.edu

Authors

Arvin Honari − *Department of Bioengineering, Erik Jonsson School of Engineering, The University of Texas at Dallas, Richardson, Texas 75080, United States;* orcid.org/0000-0001-9945-3066

Pallavi S. Kapilavaih − *Department of Bioengineering, Erik Jonsson School of Engineering, The University of Texas at Dallas, Richardson, Texas 75080, United States*

Nasrin Akter − *Department of Bioengineering, Erik Jonsson School of Engineering, The University of Texas at Dallas, Richardson, Texas 75080, United States*

Complete contact information is available at: https://pubs.acs.org/10.1021/acsapm.1c01562

Author Contributions

Conceptualization, A.H. and S.R.S.; methodology, A.H., P.S.K., and N.A.; formal analysis, A.H.; investigation, A.H.; resources, S.R.S.; data curation, A.H.; writing—original draft preparation, A.H.; writing—review and editing, S.R.S.; funding acquisition, S.R.S. All authors have read and agreed to the published version of the manuscript.

Funding

The work performed in this study has been supported by the National Institute of Health through the NCI (R01CA235756).

Notes

The authors declare no competing financial interest.

■ ACKNOWLEDGMENTS

We acknowledge Muskan Pawar for her help in acquiring scanning electron microscopy images.

■ ABBREVIATIONS

CT	computed tomography
MC	microcapsule
MRI	magnetic resonance imaging

PLA polylactic acid
PLGA poly lactic-*co*-glycolic acid
PPG propylene glycol
RFU relative fluorescence units
UCA ultrasound contrast agent
US ultrasound

REFERENCES

(1) De Geest, B. G.; De Koker, S.; Sukhorukov, G. B.; Kreft, O.; Parak, W. J.; Skirtach, A. G.; Demeester, J.; De Smedt, S. C.; Hennink, W. E. Polyelectrolyte Microcapsules for Biomedical Applications. *Soft Matter* **2009**, *5* (2), 282−291.
(2) Wang, F.; Xiao, J.; Chen, S.; Sun, H.; Yang, B.; Jiang, J.; Zhou, X.; Du, J. Polymer Vesicles: Modular Platforms for Cancer Theranostics. *Adv. Mater.* **2018**, *30* (17), 1705674.
(3) Leighton, T. G.; Apfel, R. E. The Acoustic Bubble. *J. Acoust. Soc. Am.* **1994**, *96* (4), 2616.
(4) Neppiras, E. A. Acoustic Cavitation. *Phys. Rep.* **1980**, *61* (3), 159−251.
(5) Apfel, R. E. Acoustic Cavitation: A Possible Consequence of Biomedical Uses of Ultrasound. *Br J. Cancer Suppl* **1982**, *5*, 140−146.
(6) El-Sherif, D. M.; Wheatley, M. A. Development of a Novel Method for Synthesis of a Polymeric Ultrasound Contrast Agent. *J. Biomed. Mater. Res., Part A* **2003**, *66A* (2), 347−355.
(7) Narayan, P.; Wheatley, M. A. Preparation and Characterization of Hollow Microcapsules for Use as Ultrasound Contrast Agents. *Polym. Eng. Sci.* **1999**, *39* (11), 2242−2255.
(8) Eisenbrey, J. R.; Burstein, O. M.; Kambhampati, R.; Forsberg, F.; Liu, J.-B.; Wheatley, M. A. Development and Optimization of a Doxorubicin Loaded Poly(Lactic Acid) Contrast Agent for Ultrasound Directed Drug Delivery. *J. Controlled Release* **2010**, *143* (1), 38−44.
(9) Bartolomeo, A.; Dicker, S.; Dierkes, J.; Wrenn, S. P. Nesting Microbubbles: Influence on Acoustic Activity and Image Brightness. *null* **2012**, *4* (2), 78−84.
(10) Wrenn, S.; Dicker, S.; Small, E.; Mleczko, M. Controlling Cavitation for Controlled Release. In *IEEE International Ultrasonics Symposium*; IEEE: Piscataway, NJ, 2009; pp 104−107.
(11) Peng, Y.; Seekell, R. P.; Cole, A. R.; Lamothe, J. R.; Lock, A. T.; vandenBosch, S.; Tang, X.; Kheir, J. N.; Polizzotti, B. D. Interfacial Nanoprecipitation toward Stable and Responsive Microbubbles and Their Use as aResuscitative Fluid. *Angew. Chem., Int. Ed.* **2018**, *57* (5), 1271−1276.
(12) Peng, Y.; Peng, C.; Nguyen, T.; Sun, T.; Porter, T.; McDannold, N.; Kheir, J. N.; Polizzotti, B. D. Engineering Caged Microbubbles for Controlled Acoustic Cavitation and Pressure Sensing. *ACS Materials Lett.* **2021**, *3* (7), 978−987.
(13) Gubernator, J. Active Methods of Drug Loading into Liposomes: Recent Strategies for Stable Drug Entrapment and Increased in Vivo Activity. *Expert Opin Drug Deliv* **2011**, *8* (5), 565−580.
(14) Li, D. S.; Schneewind, S.; Bruce, M.; Khaing, Z.; O'Donnell, M.; Pozzo, L. Spontaneous Nucleation of Stable Perfluorocarbon Emulsions for Ultrasound Contrast Agents. *Nano Lett.* **2019**, *19* (1), 173−181.
(15) Lepeltier, E.; Bourgaux, C.; Couvreur, P. Nanoprecipitation and the "Ouzo Effect": Application to Drug Delivery Devices. *Adv. Drug Delivery Rev.* **2014**, *71*, 86−97.
(16) Battino, R.; Rettich, T. R.; Tominaga, T. The Solubility of Nitrogen and Air in Liquids. *J. Phys. Chem. Ref. Data* **1984**, *13* (2), 563−600.
(17) Kutsche, I.; Gildehaus, G.; Schuller, D.; Schumpe, A. Oxygen Solubilities in Aqueous Alcohol Solutions. *J. Chem. Eng. Data* **1984**, *29* (3), 286−287.
(18) Heymann, M.; Panitz, F.; Rühling, K.; Felsmann, C. Solubility Coefficients for Solar Liquids, a New Method to Quantify Undissolved Gases and Practical Recommendations. *Energy Procedia* **2014**, *48*, 721−730.
(19) Lehermeier, H. J.; Dorgan, J. R.; Way, J. D. Gas Permeation Properties of Poly(Lactic Acid). *J. Membr. Sci.* **2001**, *190* (2), 243−251.
(20) Maherani, B.; Arab-Tehrany, E.; Kheirolomoom, A.; Geny, D.; Linder, M. Calcein Release Behavior from Liposomal Bilayer; Influence of Physicochemical/Mechanical/Structural Properties of Lipids. *Biochimie* **2013**, *95* (11), 2018−2033.
(21) Leelarasamee, N.; Howard, S. A.; Malanga, C. J.; Ma, J. K. A Method for the Preparation of Polylactic Acid Microcapsules of Controlled Particle Size and Drug Loading. *J. Microencapsul* **1988**, *5* (2), 147−157.
(22) Gallo, M.; Magaletti, F.; Casciola, C. M. Heterogeneous Bubble Nucleation Dynamics. *J. Fluid Mech.* **2021**, *906*, A20.
(23) Bankoff, S. G. Entrapment of Gas in the Spreading of a Liquid over a Rough Surface. *AIChE J.* **1958**, *4* (1), 24−26.
(24) Jones, S. F.; Evans, G. M.; Galvin, K. P. The Cycle of Bubble Production from a Gas Cavity in a Supersaturated Solution. *Adv. Colloid Interface Sci.* **1999**, *80* (1), 51−84.
(25) Jones, S. F.; Evans, G. M.; Galvin, K. P. Bubble Nucleation from Gas Cavities — a Review. *Adv. Colloid Interface Sci.* **1999**, *80* (1), 27−50.
(26) Lubetkin, S. D. The Fundamentals of Bubble Evolution. *Chem. Soc. Rev.* **1995**, *24* (4), 243.
(27) Sides, P. J. Phenomena and Effects of Electrolytic Gas Evolution. In *Modern Aspects of Electrochemistry*; White, R. E., Bockris, J. O., Conway, B. E., Eds.; Springer: Boston, 1986; Vol. *18*; pp 303−354.
(28) Karthika, S.; Radhakrishnan, T. K.; Kalaichelvi, P. A Review of Classical and Nonclassical Nucleation Theories. *Cryst. Growth Des.* **2016**, *16* (11), 6663−6681.
(29) Frenkel, J. A General Theory of Heterophase Fluctuations and Pretransition Phenomena. *J. Chem. Phys.* **1939**, *7* (7), 538−547.

https://doi.org/10.1021/acsapm.1c01562
ACS Appl. Polym. Mater. 2022, 4, 773−780